Real-Time Ground Reaction Force and Knee Extension Moment Estimation During Drop Landings Via Modular LSTM Modeling and Wearable IMUs

Article *in* IEEE Journal of Biomedical and Health Informatics · April 2023

DOI: 10.1109/JBHI.2023.3268239

CITATIONS
6

READS
137

5 authors, including:

Dongxuan Li
Shanghai Jiao Tong University
7 PUBLICATIONS **21** CITATIONS
SEE PROFILE

Bingfei Fan
Zhejiang University of Technology
24 PUBLICATIONS **342** CITATIONS
SEE PROFILE

Tian Tan
Stanford University
19 PUBLICATIONS **194** CITATIONS
SEE PROFILE

Real-time ground reaction force and knee extension moment estimation during drop landings via modular LSTM modeling and wearable IMUs

Tao Sun, Dongxuan Li, Bingfei Fan, Tian Tan, and Peter B. Shull *Member, IEEE*

***Abstract*— Objective: This work investigates real-time estimation of vertical ground reaction force (vGRF) and external knee extension moment (KEM) during single- and double-leg drop landings via wearable inertial measurement units (IMUs) and machine learning. Methods: A real-time, modular LSTM-based model with four sub-deep neural networks was developed to estimate the vGRF and KEM from wearable IMUs. Sixteen subjects wore eight IMUs on the chest, waist, right and left thighs, shanks, and feet and performed drop landing trials. Ground embedded force plates and an optical motion capture system were used to capture lower extremity biomechanics for model training and evaluation. Results: During single-leg drop landings, accuracy for the vGRF and KEM estimation was R^2=0.88±0.12 and R^2=0.84±0.14, respectively, and during double-leg drop landings, accuracy for the vGRF and KEM estimation was R^2=0.85±0.11 and R^2=0.84±0.12, respectively. The best vGRF and KEM estimations of the model with the optimal LSTM unit number (130) require eight IMUs placed on the eight selected locations during single-leg drop landings. During double-leg drop landings, the best estimation on a leg only needs five IMUs placed on the chest, waist, and the leg's shank, thigh, and foot. Conclusion: The proposed modular LSTM-based model with optimally-configurable wearable IMUs can accurately estimate vGRF and KEM in real-time with relatively low computational cost during single- and double-leg drop landing tasks. Significance: This investigation could potentially enable in-field, non-contact anterior cruciate ligament injury risk screening and intervention training programs.**

***Index Terms*— Machine learning, anterior cruciate ligament, landing, wearable sensors, kinetics.**

I. Introduction

Landing technique is an important skill across a spectrum of competitive sports, including basketball, volleyball, and handball [1], [2]. Landings typically induce high ground reaction forces (GRF) on the feet and produces more prominent peak knee moments than standing, walking, or running [3]–[5]. Vertical GRF (vGRF) and external knee extension moment (KEM, produced by external forces (i.e., GRF and gravity)) during landing tasks are crucial biomechanical indicators of non-contact anterior cruciate ligament (ACL) injury risk [3], [6], [7]. vGRF and KEM are typically measured in specialized laboratories using optical motion capture systems and force plates. This traditional measurement method is expensive and complex. It also limits widespread and in-field ACL-related implementations/applications, such as ACL-injury risk screening, intervention training for ACL-injury risk reduction, and real-time control of active assistive devices on the knee [8], [9]. Real-time estimation of biomechanical variables can be used to generate biofeedback, which is essential for retraining programs as they enable subjects to recognize their landing abnormalities through real-time feedback [8], [10], [11]. Also, a real-time estimation can be potentially used in the control of active assistive devices on knee joints [9].

Some physical models have been developed to estimate biomechanical variables. Tibial acceleration has been widely used as a surrogate measure of impact loading. This approach can be called "acceleration-similarity model" because the acceleration value has a similar profile as the loading rate [12]–[15]. Although the acceleration-similarity model is easy to operate and relies on fewer sensors (e.g., a single IMU), the approach generally has low accuracy (correlation coefficient of $0.44 - 0.66$ [15]). To achieve higher estimation accuracy, complex physical models, i.e., segment-link models, have been proposed for different activities including walking and ski jumping [16]–[18]. Segment-link models simplify the human body or lower limbs as rigid links without considering detailed and individual segment characteristics. The segment-link models derive kinetics from Newton-Euler equations. With accurate kinematics parameter values (derived from IMU sensors) and anthropometric data (i.e., mass, center of mass, radii of gyration ratios, and inertia [17], [19]), the segment-link models can exhibit promising estimation accuracy, the parameter values are often determined from older data sets [19].

To overcome the drawbacks of physical models, data-driven modeling methodologies have been proposed to esti-

This work was supported by the National Natural Science Foundation of China under Grant 52250610217.

The authors are with the State Key Laboratory of Mechanical System and Vibration, School of Mechanical Engineering, Shanghai Jiao Tong University, Shanghai 200240, China. Bingfei Fan is also with the college of mechanical engineering, Zhejiang University of Technology, hangzhou 310014, China (e-mail: suntao.hn@sjtu.edu.cn; sjtu_dongxuanli@sjtu.edu.cn; bingfeifan@zjut.edu.cn; alantantian@sjtu.edu.cn; pshull@sjtu.edu.cn) (*Corresponding author: Peter B. Shull*).

mate biomechanical variables, such as loading rate [15], GRF [1], [20]–[22], and knee moments [23], [24] in walking and running, using inexpensive and portable wearable inertial measurement units (IMUs). Unlike periodic walking and running movements, drop landings are characterized by large, non-periodic, and short-term impacts. These features require drop landing estimation models to have a faster response and higher stability to cope with the special impacts. Therefore, drop landings require distinctive IMU models that are specifically tailored to capture landing characteristics.

Two primary approaches have been proposed for estimating the vGRF and KEM during drop landings. A multiple-feature linear regression model combined with two IMUs was proposed by Chaaban et al. [25] to predict peak vGRF, peak knee flexion angle, peak KEM, and peak sagittal knee power absorption during double-leg jump landings. The model was trained with empirically selected features extracted from accelerations and angular velocities measured by the IMUs worn on the shank and thigh of subjects. Although the model was efficient, it could only estimate the peak values of the variables. In addition, the estimation process was offline and the input features needed to be extracted from the whole drop landing period at once. Another model was developed by Cerfoglio et al. [26] using the nonlinear autoregressive network with external input (NARX). The model inputted with IMUs was able to estimate the three-dimensional GRF and knee moment profiles. The NARX is a recurrent dynamic neural network with feedback connections enclosing several neural network layers, which can map the nonlinear and complex relationship between IMU signals and the GRF and knee moments. However, the model requires force plate measurements to determine the landing phase, and it cannot be executed in real time. Additionally, although the model could predict three-dimensional GRF and knee moment, it was designed with a complex structure (i.e., 2006 neurons in hidden layers), thereby requiring a lot of computation resources or having high time-complexity. Also, the existing research of landing biomechanical estimations only focused on the specific target variables during double-leg drop landings [25], [26], while single-leg drop landings, which have a higher injury risk than double-leg [3], have not been investigated so far. To sum up, the two primary approaches for ACL-related assessment are currently limited by several factors, including inability to predict the whole profile of the variables or dependencies on non-wearable equipment, lack of real-time estimation, and the fact that it is not applicable to single-leg drop landings [25], [26]. Therefore, a concise estimation model that can efficiently and in real-time predict required variables during single- and double-leg drop landings would be more beneficial for practical ACL-related applications.

The number and locations of wearable IMUs and model complexity can also significantly affect estimation accuracy of the vGRF and KEM. For example, a shank-worn IMU has been demonstrated to be significantly more accurate than the IMUs placed on the other body segments when estimating the loading rate of the vGRF during running [15]. For drop landing tasks, only shank and thigh have been selected for placing IMUs [25], [26]. However, chest (or trunk) and pelvis flexion angles, as well as toe direction would influence non-contact ACL injury risk in drop landings due to their association with knee biomechanics [6], [27], [28]. It is unclear whether incorporating IMUs placed on the chest, waist, and feet could significantly influence the vGRF and KEM estimation accuracy.

The primary limitation of current approaches is that existing estimation models of the vGRF and KEM during drop landings are not in real time and cannot be applied to single-leg drop landings. Therefore, this study proposed a modular long short-term memory (LSTM)-based model that uses body-worn IMUs to estimate the vGRF and KEM in real time during single- and double-leg drop landings.

II. Methods

A. Modular LSTM-based model for real-time estimation

A modular LSTM-based model combined with wearable IMUs was developed to estimate the vGRF and KEM in real time during single- and double-leg drop landings (Fig. 1). The model has three components: (1) a drop landing event detection module to identify the region of interest (ROI) of a drop landing movement based on IMU acceleration magnitudes, (2) a time-window buffer to store and transferring IMU data, and (3) four small-sized sub-networks to map normalized IMU signals to the target variables (i.e., the vGRF and KEM). Drop landing ROI is defined as a short but complete period of the drop landing motion for the estimation. The four sub-networks have the same structures which were trained to estimate the different target variables. The model is modular in that the sub-networks can predict different variables by activating the corresponding sub-networks, thus saving computational resources in portable applications.

A subject's motion states during drop landings, such as take-off, flight phase, landing, and stance phase, can be estimated using the acceleration of a subject's body [21], [29]. When the magnitude is less than gravitational acceleration, the subject is in flight phase [21] and when the magnitude increases to several times gravitational accelerations, the subject touches the ground [29]. These principles can be adapted to determine the flight phase and landing event of drop landings as follows:

$$\text{motion state} = \begin{cases} \text{flight phase}, & \|g_{imu}\| < \alpha\|g_0\| \\ \text{landing event}, & \|g_{imu}\| > \beta\|g_0\| \\ \text{pre-flight or post-landing}, & \text{others} \end{cases}, \tag{1}$$

where $\|g_{imu}\|$ and $\|g_0\|$ denote the magnitudes of the IMU and gravitational accelerations, respectively. α is a coefficient to compensate the IMU accelerations induced by the subject's segment movement in the air. α was empirically set to 0.5 in the following experiments. β is a threshold coefficient of landing accelerations and was set to 5 following [29].

The drop landing event detection module can real-time monitor the changes in the acceleration magnitude of an IMU (i.e., placed on the chest) to automatically identify the beginning and end moment of the ROI (1). The start of the ROI occurs in the flight phase, which is identified when

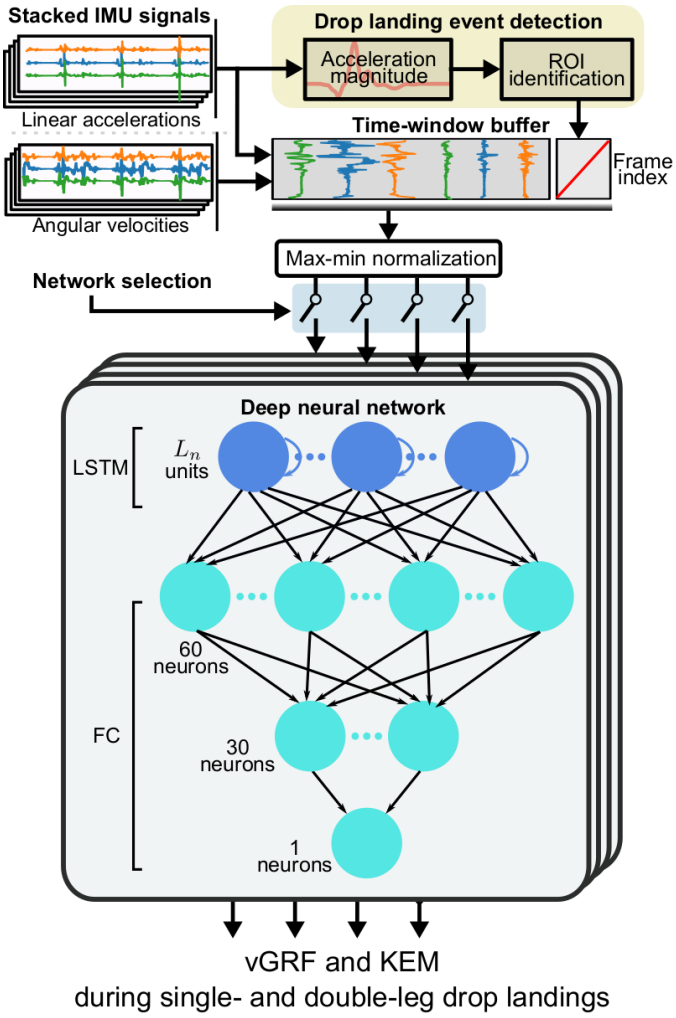

Fig. 1. Architecture of the proposed modular LSTM-based model for real-time estimation of the vGRF and KEM. The model identifies the region of interest (ROI) of the drop landings based on IMU acceleration magnitudes. Meanwhile, the IMU data are stored in a time-window buffer. When the ROI is identified, the buffered data are transferred into one of four identical deep neural networks for predicting target variables. The model is modular and it can be configured to output the vGRF or KEM during single- or double-leg drop landings by activating the different neural networks.

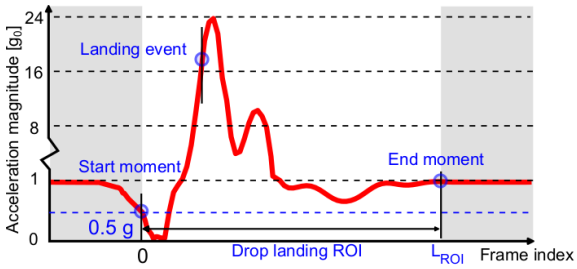

Fig. 2. Graphical interpretation of identifying the ROI during a drop landing task. The start moment of the ROI is identified when the acceleration magnitude of an IMU reduces to less than $\mathbf{0.5}\|\boldsymbol{g}_0\|$. The frame of IMU data is indexed as zero at the start moment. After a landing event happens (1) and the frame index increases to $\boldsymbol{L_{ROI}}$, the drop landing ROI is fulfilled. The start and end moments define the period of ROI, which includes the landing moment inside.

the acceleration magnitude is smaller than $\alpha\|g_0\|$ (Fig. 2). From the moment, the IMU data are regarded as valuable inputs and fed to the model. Each frame of IMU data is indexed and update from zero. After a landing event happens ($\|g_{imu}\| > \beta\|g_0\|$) and the frame index number reaches L_{ROI} that defines the length of the drop landing ROI, a complete drop landing period is fulfilled. L_{ROI} was empirically set to 80 frames (0.8 s) so that the landing moment was inside the ROI in the following experiments. In the presence of sensor noise in acceleration, the identified start, landing, and end moments of the ROI may deviate from their true positions, thereby leading to an offset in the detected ROI. However, the threshold coefficients (α and β) offer sufficient tolerance for the effect of the noise. As a result, the accuracy of the ROI detection was ensured.

The time-window buffer receives each frame of the IMU data and slides over the entire drop landing ROI. The buffer stores the current and three previous frames of IMU data and stacks the frame index. Every four frames of the IMU data and frame index are normalized and transferred to the selected neural networks through the switch channels.

Each neural network contains an LSTM layer with L_n units and three fully-connected (FC) layers with 60, 30, and one neurons, respectively. The LSTM layer can effectively process temporal inputs to obtain the complex and dynamic relationship between the IMU data and the target variables (i.e., the vGRF and KEM) [30]. The outputs of the LSTM layer are transferred to the normalized target variables (GRF or KEM) by the three FC layers. The activations of neurons in the three FC layers are rectified linear unit (ReLU), ReLU, and tanh, respectively.

The model was trained and tested based on a leave-one-subject-out cross-validation method such that all data from one subject were used for testing while the data from the remaining subjects were used for training [23], [31]. The LSTM and FC neural networks of the model were implemented using Keras (version 2.5.0), a high-level neural networks application programming interface (API) in Python. Low-level operations were performed in TensorFlow (version 2.5.0), which interfaced with Keras. The Glorot normal initializer was used to initialize the LSTM cell state and FC layer neurons, and the stochastic gradient descent with momentum optimizer was used to optimize the training process. The dropout layer was used in the training process to avoid over-fitting. Max-min normalization was used to normalize each IMU channel. The normalization parameter values were determined by the training data, and the same parameter values were applied to the testing data. The model is modular and it can be configured to predict different variables of single- and double-leg drop landings by selecting the corresponding sub-network.

B. Participants

Sixteen males with no history of musculoskeletal disorders were recruited to perform single- and double-leg drop landing tasks to collect dataset for model training and evaluation. Average and standard deviation of age, height, and weight were 23.2 ± 1.4 years, 1.77 ± 0.04 m, and 72.8 ± 9.7 kg, respectively. All subjects provided written informed consent

prior to testing, and the experimental procedure was reviewed and pre-approved by the university ethics committee under No. E2021013P.

C. Experimental protocol

The drop landing experiments to collect the dataset were conducted in a biological laboratory equipped with a ten-camera optical motion capture system (100 Hz, Vicon™, UK) and two side-by-side force plates (1000 Hz, AMTI™, USA) embedded in the floor (Fig. 3 (a)). During drop landings, the optical motion capture system and embedded force plates were used to acquire subjects' kinematics and GRF. The measurements were used as the ground truth of the model output in model training and evaluation. The model inputs were motion-related segments' accelerations and velocities. For the vGRF and KEM estimations, the motion-related segments typically were the chest, waist, thighs, shanks, and feet [15]. Thus, eight wearable IMUs (Xsens Technologies B.V., Enschede, The Netherlands) were placed on the segments to collect their accelerations and angular velocities. The values were as features by the model to make estimations for the vGRF and KEM of the leg (Fig. 3 (b)). The measurements of the optical motion capture system, force plates, and IMU system were synchronized via RCA sync cables which connected the three systems to start recording data simultaneously.

To facilitate the implementation of the proposed estimation model, IMUs were manually placed without installation calibrations. The reference anatomical locations of the IMUs were (Fig. 3 (b)): trunk–fifth thoracic vertebrae, pelvis–mid-point between left and right anterior superior iliac spine, left and right thigh–mid-point between the left anterior superior iliac spine and left femur medial epicondyle, left and right shank–one third point between left femur medial epicondyle and left tibia apex of medial malleolus near proximal end of tibia, and left and right foot–left second metatarsal [32]. The IMUs' placement orientation follows the principles: The IMUs' z-axes were perpendicular to the skin surface and y-axes were vertical upward during standing except for the IMUs on the feet whose y-axes were from the anterior to the posterior.

We placed 32 reflective markers on anatomical landmarks according to the Visual3D[1] full-body model[2] (Fig. 3 (b)): calcaneus (LFCC and RFCC), head of the second metatarsal (LFM2 and RFM2), head of the fifth metatarsal (LFM5 and RFM5), lateral and medial malleoli (LFAL, LTAM, RFAL, and RTAM), lateral and medial femoral epicondyles (LFLE, LFME, RFLE, and RFLE), tibial tuberosity (LTT and RTT), lateral mid-shaft shank (LSK and RSK), greater trochanter (LFT and RFT), lateral mid-shaft femur (LTH and RTH), left and right ilium crest tubercle (LIAS and RIAS), left and right posterior superior iliac spines (LIPS and RIPS), sternum jugular notch (SJN), left and right acromion (LAC and RAC), seventh cervical vertebra (CV7), sternum xiphisternal joint

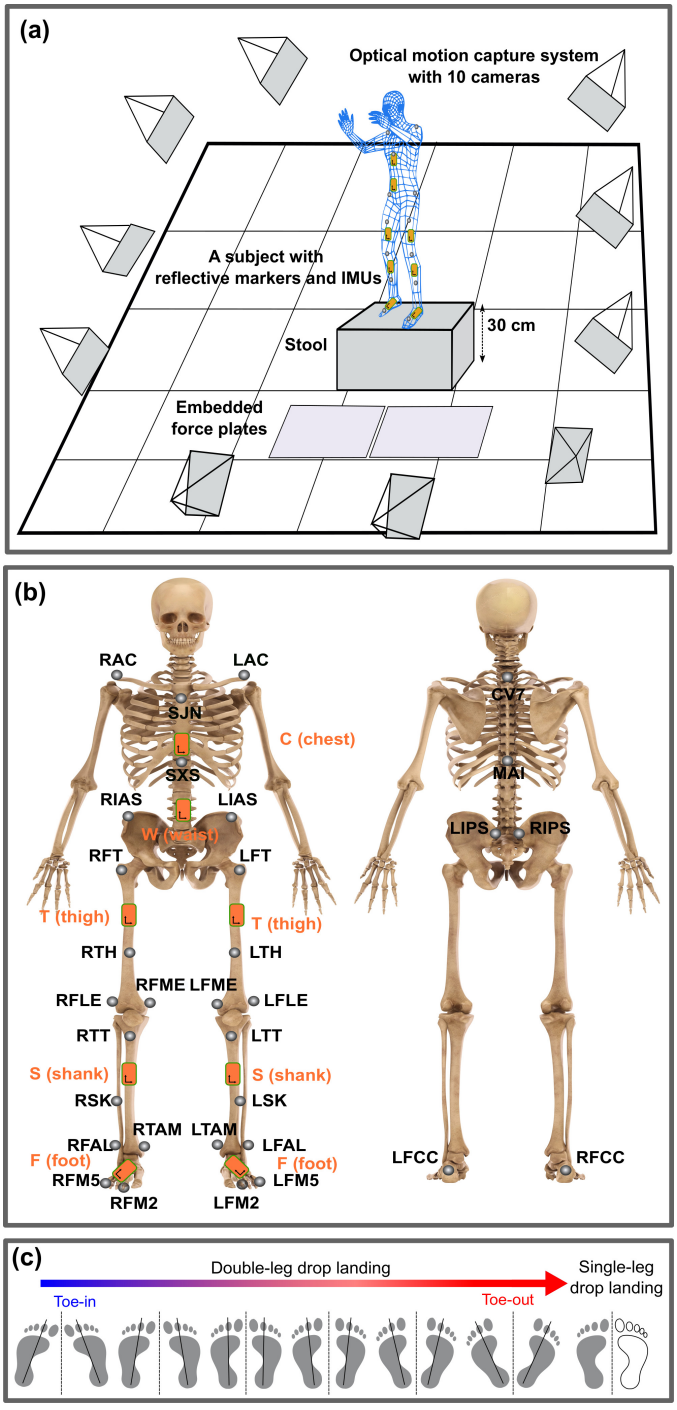

Fig. 3. Experiment setup. (a) A biomechanical laboratory with an optical motion capture system and two side-by-side embedded force plates were used to measure drop landing tasks. Subjects were instructed to land on the force plates from a 30-cm-high stool. (b) Thirty-two reflective markers were pasted on the subjects' anatomical landmarks. Eight IMUs were strapped to the chest, waist, and both thighs, shanks, and feet. (c) Each subject performed 30 double-leg drop landing tasks with six different toe directions from toe-in to toe-out and 15 single-leg drop landing tasks.

[1] https://www.c-motion.com/

[2] https://c-motion.com/v3dwiki/index.php?title=Marker_Set_Guidelines

(SXS), and midway between the inferior angles of most caudal points of the two scapulae (MAI).

Each subject wore standard athletic shoes (Revolution 4, Nike, Inc., Beaverton, USA) and was instructed to jump forward from a 30-cm-high stool to the embedded force plates, landing on both legs or a single leg (Fig. 3 (a)). Valid double-leg drop landing trials were repeated 30 times with six different toe directions: a self-selected toe direction and five toe directions from toe-in to toe-out in individual acceptable toe direction ranges (Fig. 3 (c)). Each toe direction condition had five trials. The aim of varying the toe direction was to produce various landing kinetics to increase the generalisability of the data set. Afterward, each subject performed single-leg drop landing trials, in which 15 valid trials were collected. From a safety aspect, the subjects were not asked to manipulate the toe direction during single-leg drop landings. The optical motion capture system, force plates, and eight IMUs were synchronized to collect the dataset for model training and evaluation.

D. Data processing

The vGRF measured by the force plates were down-sampled from 1000 Hz to 100 Hz and filtered at 15 Hz using a zero-lag second-order low-pass Butterworth filter [33]. A threshold of 20 N in the vGRF was used to determine the initial foot-ground contact. To calculate the KEM, we built a biomechanical model for each subject in Visual3D using the data measured by the optical motion capture system and force plates (Fig. 4). The biomechanical model could output the KEM that was also filtered with a zero-lag second-order low-pass Butterworth filter at 15 Hz. The filtered vGRF and KEM were regarded as ground truth in model training and evaluation processes. To reduce the influence of varied subjects' weights and heights on model training and performance assessment, the vGRF and KEM were normalized. The vGRF was divided by the body weight (BW), while the KEM was divided by the multiplication of BW and body height (BH). The linear accelerations and angular velocities of the eight wearable IMUs were also filtered using a zero-lag second-order low-pass Butterworth filter with a 15-Hz cut frequency. Finally, the linear accelerations and angular velocities from different IMUs were stacked as needed before being transferred to the model.

E. Performance evaluation

vGRF and KEM are highly related to thigh, shank, foot, waist, and chest during landing tasks [3], [25], [26]. Thus IMUs were placed at these five segments. The other leg's motion state could also influence the leg's estimation accuracy, especially during single-leg drop landings, there were three additional IMUs placed at the other leg's foot, shank, and thigh. In the results, we used the right leg (R) as an example to explore the model performance. There are 31 ($\sum_{n=1}^{5} C_5^n$) ways to select one to five IMUs on the right leg's five typical locations for feature collections in total (i.e., right leg's foot (RF), shank (RS), and thigh (RT), and waist (W), and chest (C)). We also explored the influence of the five typical IMU locations with the one to three additional IMU locations on the estimation accuracy (i.e., left leg's foot (LF), shank (LS), and thigh (LT)).

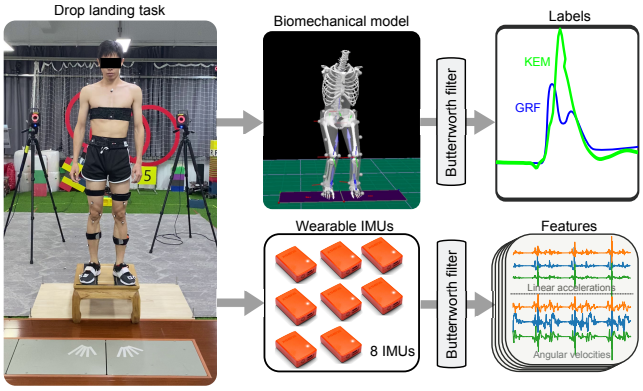

Fig. 4. The experiment data were measured by synchronizing the optical motion capture system, embedded force plates, and wearable IMUs and post-processed for model training and evaluation. Each subject's biomechanical model was created to calculate the vGRF and KEM as the ground truth. IMUs' acceleration and velocities were low-pass filtered to be the model inputs.

In addition to the IMU configurations (IMU number and locations), the LSTM unit number (L_{LSTM}), which determines the model complexity and execution time, also affects the model estimation accuracy. To clarify the influences of the IMU configurations and LSTM unit number on the model performance, we trained and tested the model under different IMU and LSTM unit numbers and compared their performance to find an optimal IMU number and an optional LSTM unit number. The execution time of the model under different LSTM unit numbers was also explored to verify whether the estimation can be launched in real time concerning the IMUs with a 100 Hz sampling frequency. The root mean square error (RMSE), relative RMSE (rRMSE), and coefficient of determination (R^2) between ground truth and estimated values were employed to assess the model performance. We referenced similar algorithm development [25], [34], which defined $R^2 > 0.80$ as high algorithm accuracy. R^2 was mainly used in the investigation of different IMU configurations and LSTM unit numbers. In the summary of the results, the RMSE and rRMSE were used to demonstrate the performance of the models. Besides, we implemented a t-test to determine whether IMU number and location affect the vGRF and KEM estimation accuracy. Note that the assessment of the optimal LSTM unit number and IMU configuration was demonstrated by the vGRF estimation of the right leg during double-leg drop landings as an example.

III. Results

A. Estimation results with optimized IMU configurations and LSTM unit number

The vGRF and KEM estimation of the right leg during single- and double-leg drop landings can be seen in Fig. 5. In the estimations, the model had optimized IMU configurations and an optimal LSTM unit number ($L_n = 130$). Each ensemble curve in the figure was plotted using 431 and 150 cross-validation tests of the double- and single-leg drop landing

trials, respectively. The estimated vGRF and KEM can match their actual (measured) values well except for the peak values. The estimation errors during the drop landing mainly occurred at the peak points.

An overview of the estimation performance for the vGRF and KEM during single- and double-leg drop landings was presented in Table I. Compared to the non-optimized IMU configurations, the model with optimal IMU configurations showed greater estimation accuracy (Tables I and II). Note that several estimation results with outlier accuracy (i.e., $R^2 < 0.4$) were removed from the performance assessment. The optimized IMU configurations for the four target variables were different. During the single-leg drop landings, the model with seven IMUs (placed the right leg' foot, shank, thigh, the left leg's foot, shank, the chest, and waist) or all eight IMUs exhibited the highest mean accuracy, $R^2 = 0.88 \pm 0.12$ and $R^2 = 0.84 \pm 0.14$ for the vGRF and KEM estimations, respectively. During double-leg drop landings, the model with only four IMUs (placed on the right leg's foot, shank, thigh, and chest) and five IMUs (placed on the right leg's foot, shank, thigh, chest, and waist) exhibited the highest accuracy, $R^2 = 0.85 \pm 0.11$ and $R^2 = 0.84 \pm 0.12$ for the vGRF and KEM estimations, respectively. The accuracy of 50% and 25% estimations were large than 0.87 and 0.92, respectively. Some estimations had very low accuracy ($R^2 < 0.5$). This is probably because those trials were influenced by different factors, such as loose IMU attachment.

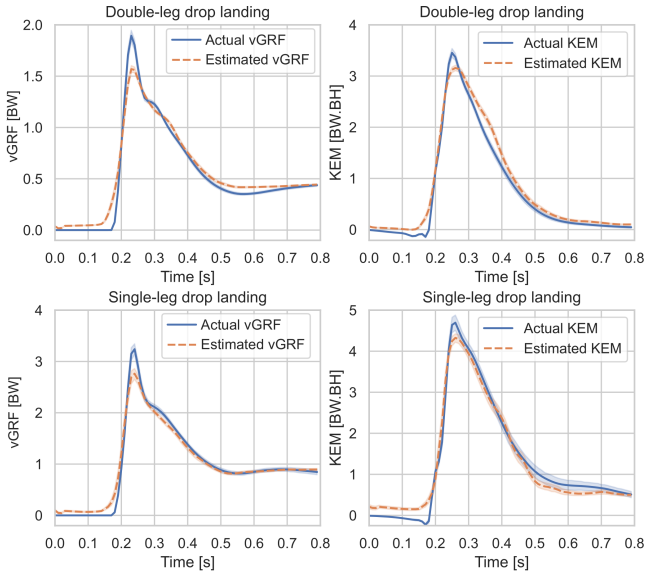

Fig. 5. Ensemble curves of the vGRF and KEM estimations during double- and single-leg drop landings. The actual (measured) and predicted vGRF and KEM are shown as the solid and dashed lines, respectively.

B. Influence of LSTM units and IMU number

We compared the estimation accuracy of the model under nine different LSTM unit numbers (i.e., 1, 25, 50, 75, 100, 125, 150, 175, and 200) and eight IMU numbers (i.e., 1, 2, 3, 4, 5, 6, 7, and 8). The vGRF estimation accuracy of the right leg during double-leg drop landings, as an example, was used

TABLE I

ESTIMATION PERFORMANCE OF THE RIGHT LEG FOR THE VGRF AND KEM WITH OPTIMIZED IMU CONFIGURATIONS DURING SINGLE- AND DOUBLE-LEG DROP LANDINGS. THE UNITS OF RMSE FOR VGRF AND KEM WERE BW AND BW · BH, RESPECTIVELY.

Variables	IMU configurations	Metrics	Mean	Min	25%	50%	75%	Max
Single-leg vGRF	RF, RS, RT, W, C, LF, LS [a]	R^2	0.88 ± 0.12	0.45	0.87	0.93	0.96	0.99
		rRMSE	0.07 ± 0.04	0.02	0.05	0.06	0.09	0.18
		RMSE	0.25 ± 0.13	0.08	0.17	0.21	0.29	0.73
Single-leg KEM	RF, RS, RT, W, C, LF, LS [a]	R^2	0.84 ± 0.12	0.41	0.79	0.88	0.92	0.98
		rRMSE	0.10 ± 0.04	0.05	0.08	0.10	0.12	0.23
		RMSE	0.54 ± 0.18	0.20	0.41	0.49	0.66	1.18
Double-leg vGRF	RF, RS, RT, C	R^2	0.85 ± 0.11	0.42	0.81	0.89	0.92	0.97
		rRMSE	0.08 ± 0.03	0.04	0.06	0.08	0.10	0.19
		RMSE	0.18 ± 0.06	0.08	0.14	0.17	0.21	0.37
Double-leg KEM	RF, RS, RT, C, W [b]	R^2	0.84 ± 0.12	0.45	0.80	0.87	0.92	0.98
		rRMSE	0.10 ± 0.04	0.04	0.08	0.10	0.12	0.21
		RMSE	0.38 ± 0.10	0.16	0.31	0.38	0.45	0.62

[a] The estimation accuracy of the models with seven and eight IMUs were close to each other in R^2 during single-leg drop landings.
[b] The KEM estimation accuracy of the models with five and more IMUs were close to each other in R^2 during double-leg drop landings.

to represent the comparison. The accuracy results (R^2) were regressed with a two-order polynomial method to visualize their relationship. The proposed model under the different IMU numbers all had optimal LSTM unit numbers from 100 to 150 concerning the accuracy (R^2) (Fig. 6). From one to four IMUs, the model exhibited gradually increased accuracy independence on the LSTM units, while the accuracy had no improvement from using four to seven IMUs. This indicates that adding more IMUs and using a proper LSTM unit number is an effective way to improve the estimation accuracy when the available IMU number is less than or equal to four. The optimal LSTM unit numbers of the model under all IMU numbers were close to 130 ($L_n = 130$), so this value was used in the experiments of the following results.

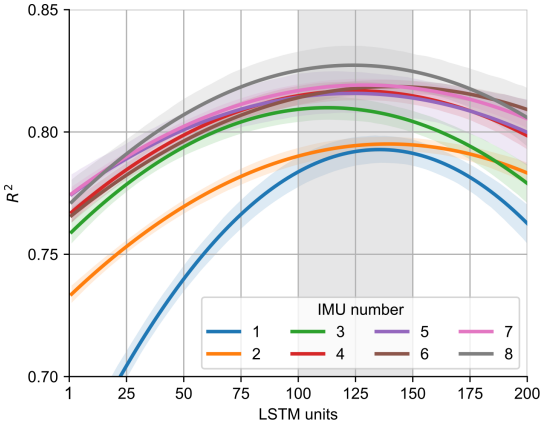

Fig. 6. The vGRF estimation accuracy ($\boldsymbol{R^2}$) of the right leg during double-leg drop landings under the model with different LSTM unit and IMU numbers. The optimal LSTM unit numbers of the model under different IMU numbers are all close to 130.

More LSTM units complicated the model and increased the time complexity of the model. The computation time of each estimation frame increased with the increase of LSTM units (Fig. 7). Note that the time cost did not include data collection and transmission of the eight IMUs. We examined

the execution time of the model when estimating the vGRF of the right leg with five IMUs during a double-leg drop landings. The estimation was executed on a personal computer (Intel(R) Xeon(R) CPU E5-2678 v3 @2.5 GHz and 8GB DDRAM) using only a single CPU core for the computation. The execution time of estimation per frame is raised slightly when using more LSTM units. The average execution time per frame was less than 10 ms. It indicated that the model can estimate the target variables in real time by using the wearable IMU having a 100 Hz sampling frequency on the personal computer without using GPU.

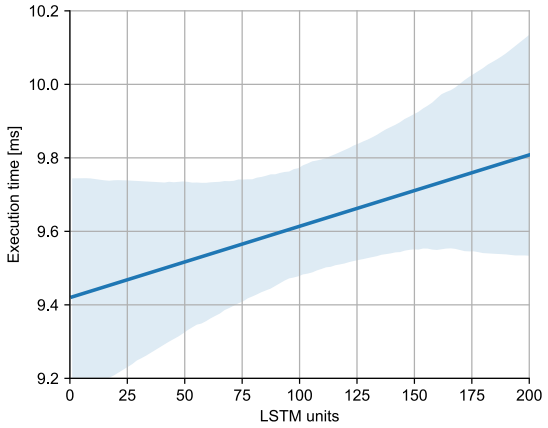

Fig. 7. Execution time of the estimation per frame increased with the increase of the LSTM units. The execution time was collected when the model with five typical IMUs launched on a personal computer (Intel(R) Xeon(R) CPU E5-2678 v3 @2.5 GHz and 8GB DDRAM)

The proposed model with more IMUs exhibited higher estimation accuracy (Fig. 8). The median estimation accuracy of the model with one to four IMUs increased significantly while the model with four to eight IMUs has no significant improvement in median accuracy. The model with four IMUs exhibited a little higher median estimation accuracy than that with more than four IMUs. The accuracy deviation of the model estimation decreased when using an increased IMU number. From the perspective of average accuracy, the model with more IMUs showed better performance. This is because the IMU locations also affect the estimation accuracy even with the same IMU number.

C. Influence of IMU locations

The locations of the IMUs on subjects also determine the feature selections and then affect the model estimation accuracy [31]. We explored the model performance with a single IMU placed on the eight IMU locations in the vGRF estimation during the double-leg drop landings (Fig. 9). Their median accuracy of the model estimation gradually increased from the left shank (LS), right foot (RF), waist (W), left foot (LF), left thigh (LT), right thigh (RT),and right shank (RS) to the chest. The median accuracy of the right thigh, right shank, and chest are significantly greater than that of other single IMU locations. The model with an IMU placed on the chest exhibited the greatest median accuracy.

For the vGRF and KEM estimation of a leg (e.g., the right leg), the other leg's (e.g., the left leg) motion state

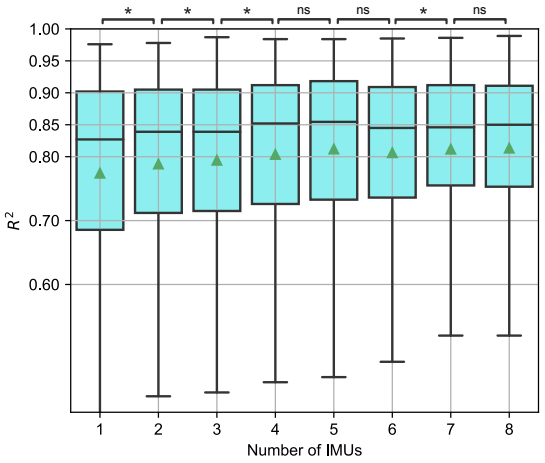

Fig. 8. The vGRF estimation accuracy ($\boldsymbol{R^2}$) of the right leg during double-leg drop landing under the model with the eight different IMU numbers. The lines and triangle points inside the boxes represent the median and mean of the accuracy, respectively. ns indicates no statistically significant difference. * denotes significant differences with p-value $\leq \mathbf{0.05}$. To perform the test, the IMU locations were sorted incrementally according to their mean and median accuracy, as shown in the figure. Consequently, it was only necessary to test adjacent conditions.

during landings could also influence the estimation accuracy. Our experiment results suggested that the left leg's foot and shank motions have more influences on the right leg's vGRF estimation than the right leg' foot motion (Fig. 9). This is the reason why the model with eight IMUs (three of the IMUs on the left leg) showed high accuracy (Fig. 8).

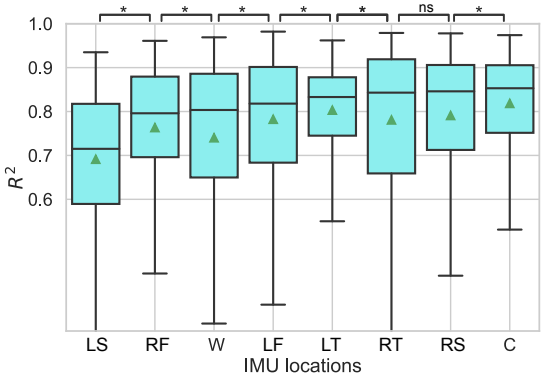

Fig. 9. The vGRF estimation accuracy of the right leg during double-leg drop landing under the model with an IMU placed on the eight IMU locations: right foot (RF), right shank (RS), right thigh (RT), waist, chest, left foot (LF), left shank (LS), and left thigh (LT). The lines and triangle points inside the boxes represent the median and mean accuracy, respectively. ns indicates no statistically significant difference. * denotes significant differences with p-value $\leq \mathbf{0.05}$. To perform the test, the IMU locations were sorted incrementally according to their mean and median accuracy, as shown in the figure. Consequently, it was only necessary to test adjacent conditions.

The optimal IMU locations of the different IMU numbers, concerning the vGRF estimation of the right leg during double-leg drop landings, can be seen in Fig. 10. When only one IMU was used in drop landing estimation, its best location for getting high accuracy was on the chest. To get the best median accuracy of a leg's vGRF estimation, four IMUs placed on the chest and the leg's thigh, shank, and foot were enough.

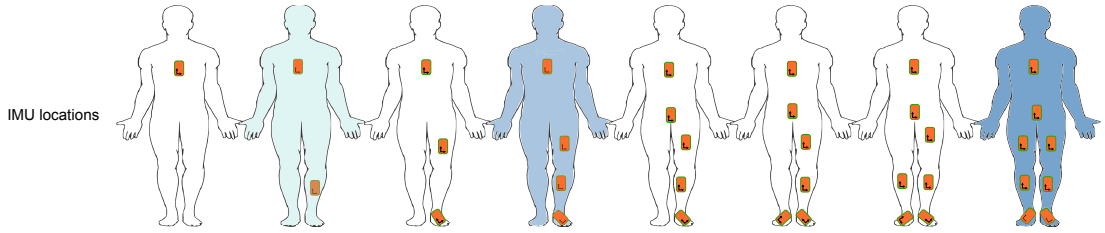

Number of IMU	1	2	3	4	5	6	7	8
Median R^2	0.85	0.87	0.84	0.87	0.85	0.87	0.86	0.87
Mean R^2	0.82 (0.11)	0.81 (0.15)	0.81 (0.11)	0.82 (0.13)	0.81 (0.12)	0.80 (0.17)	0.82 (0.13)	0.86 (0.07)
Mean RMSE (BW)	0.20 (0.07)	0.21 (0.09)	0.21 (0.07)	0.20 (0.08)	0.21 (0.08)	0.21 (0.09)	0.20 (0.08)	0.18 (0.06)
Mean rRMSE	0.09 (0.03)	0.09 (0.04)	0.09 (0.03)	0.09 (0.03)	0.09 (0.03)	0.09 (0.04)	0.09 (0.03)	0.08 (0.02)
IMU configuration priority	6	3	8	2	7	4	5	1

Fig. 10. The statistical estimation accuracy of the right leg's vGRF during double-leg drop landings under the model with one to eight optimally-placed IMUs. The IMU configuration priority provided suggestions for IMU configuration. The estimation variable is the vGRF during double-leg drop landings. BW represents body weight of subjects

The four IMUs enabled the model to have the same median accuracy as the eight IMUs except for the accuracy of the four IMUs having a relatively large deviation. From the aspect of the mean accuracy, the model with eight IMUs showed the highest accuracy and had the lowest RMSE and rRMSE. In short, the strategy of configuring the IMUs is that using all eight IMUs if there are enough IMUs, otherwise utilizing only four IMUs placed on the chest and the leg's foot, shank, and thigh (Fig. 10). We introduced IMU configuration priority to assess the IMU configuration strategy. IMU configuration strategies that exhibit high average estimation accuracy and low variance were assigned higher priority. In practical applications, these high-priority strategies should be selected first.

D. Comparison with acceleration-similarity and linear regression models

We compared the proposed method (modular LSTM model) with two existing approaches: acceleration-similarity model (a type of physical model) and linear regression model (a type of machine learning model). For the acceleration-similarity model, the tibial acceleration that measured by a wearable IMU placed on the shank was used to estimate the vGRF via a linear transfer. As an example, the acceleration of the IMU on the right shank was used to predict the right leg vGRF. The acceleration-similarity model can be expressed as:

$$F_v = w_1 \cdot A_x + w_2 \cdot A_y + w_3 \cdot A_z + b \qquad (2)$$

where F_v represents the estimated vGRF, $A_{x,y,z}$ are the tibial accelerations along with its three directions. $w_{1,2,3}$ and b are scaling and offset parameters whose values were calculated by a regression algorithm[3].

For the linear regression model, we referred to Chaaban et al. [25] who elaborated on features extracted from 3D accelerations and 3D angular velocities of two IMUs that were placed on the thigh and shank. The features were fed into a stepwise linear regression model to estimate the target variables. The features includes the maximum/minimum values of acceleration and angular velocities and their statistical indexes. A leave-one-out cross-validation was performed on the dataset that was split into 10 folds. The model was trained on 9 folds and tested on the remaining fold and repeated this process across each fold. A paired t-test was used to determine if the mean R^2 of the modular LSTM model was significantly higher than that of the acceleration-similarity and linear regression models (Fig. 11). The results showed that the modular LSTM model outperformed the linear regression model in KEM estimation and the acceleration-similarity in vGRF estimation.

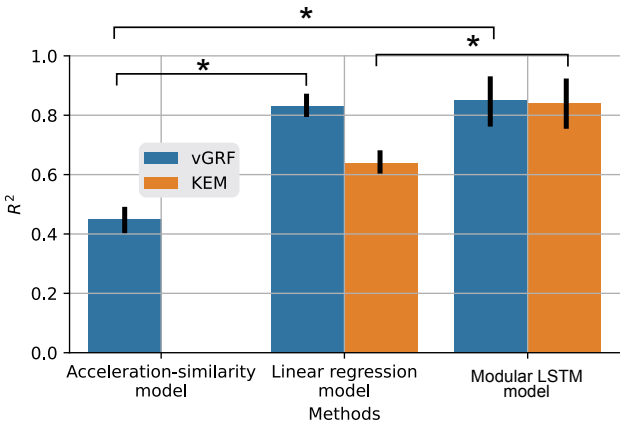

Fig. 11. Estimation accuracy comparison of our proposed method (modular LSTM model) with other two existing methods: acceleration-similarity [12] and linear regression model [25]. Note that the acceleration-similarity model was only able to estimate vGRF using our collected IMU data, while the accuracy of the linear regression model comes from [25].

IV. Discussion

This work proposed a modular LSTM-based model for real-time estimating the vGRF and KEM during drop landing tasks. We investigated the model features including model complexity using LSTM unit number and applicability for different IMU configurations and target variables. The evaluation results demonstrated that the model is modular which can be set to estimate different variables and be employed in single- and double-leg drop landings. In addition, the model has low time-

[3]The implementation of the acceleration-similarity model can be found at `https://gitlab.com/sunzhon/realtime_drop_landing_estimation.git`.

complexity and can perform the estimation in real time to process the IMU data at 100 Hz.

A. Modularity and real-time estimation

To handle the specific characteristics, larger impact, short-term, and non-period of drop landing, the proposed model has two features, modularity and real time, which are different from the existing estimation models [1], [20]–[22], [24]. First, the model is modular and can be flexibly set to be applied in different estimation applications. The existing research utilized a large and complex neural network with fixed multiple output channels to predict multiple target variables [24]–[26]. Instead, this work utilized several identical small neural networks to flexibly configure the estimation model as needed (Fig. 1). The model can output more variables by adding and training more sub-networks. We have collected the necessary dataset for training the model to predict the lower extremity biomechanics of drop landing, including 3D angles and moments of the ankle, knee, and hip joints. The dataset and code can be accessed at `https://gitlab.com/sunzhon/realtime_drop_landing_estimation.git`. The feature allows the model to be a flexible estimation module for different in-filed applications, such as ACL risk factor screening [4], assistive device monitoring and control [9], [35], since they may require different estimations. The modularity enables the model to have a small size and to require relatively low computation. Second, the model can run in real time. The model was designed to use only the current and a few history IMU data (three frames) so that the model ran online with less computation and time-saving, thereby achieving real-time estimation.

The proposed model, using eight IMUs, can update at a frequency of 100 Hz in real-time applications. In the experiments, the eight IMUs had a sampling frequency of 100 Hz and sent their data to a computer without package loss simultaneously. Also, the execution time per frame of estimation could be less than 10 ms on a personal computer. From the aspect of delay, considering the time delay in the data collection and transport of the eight IMUs, the estimation had a maximum 20 ms delay (the time cost of a frame of data communication and model computation). Although the delay is large, it would be acceptable for real-time application because there is more than 20 ms between two successive landings.

During a drop landing task, humans may not be able to make adjustments in real time (within a short period, such as 10 ms) due to humans' physical and sensory limitations. However, real-time estimation of biomechanical variables can still be important for clinicians and researchers to identify potentially harmful landing loads that can lead to injury and develop effective injury prevention and rehabilitation strategies. Subjects can receive biofeedback to recognize their landing status online, which can help them adjust their landing technique in consecutive trials. Also, although further validation of the estimation accuracy and reliability is needed before applying the proposed method in assistive devices or artificial limbs, efforts in this work were made to pave the way toward to practical applications.

B. Adaptability

The proposed model with the optimal LSTM unit number adapts to the different IMU configurations. The complexity and mapping capability of the model are determined by the LSTM unit number (L_n, Fig. 1) that plays a crucial role in modeling. A large L_n value can improve the capability of the model for explaining the IMU data, but increase the model complexity, training time, and possibility of overfitting. To find proper L_n value, we used grid search to explore the proper LSTM unit number under the different IMU configurations (Fig. 6). The results indicate that the optimal LSTM unit numbers of the model under the different IMU configurations are similar. This suggests that the proposed model with the optimal LSTM unit number under an IMU configuration will also be good on other IMU configurations. Additionally, the model can also adapt to the double-leg drop landings with the different toe directions since the training dataset of the model contained varied toe directions from toe-in to toe-out (Fig. 3 (c)).

C. IMU configurations

IMU configurations, including IMU numbers and locations on the subject, significantly influence the model estimation accuracy during single- and double-leg drop landing tasks. Unlike the conclusion that a single shank-worn IMU caused excellent accuracy of loading rate estimation during running in [15], multiple IMUs could enable the proposed machine learning model to exhibit better estimation accuracy during drop landings (Fig. 8). Specifically, unlike the best double-leg drop landing estimations with only four or five IMUs, during single-leg drop landings the best vGRF and KEM estimations of a leg relay on the IMUs on another leg. The distinction is probably because of the specific characteristics of drop landings: large, non-periodic, and short-term impact, so the model needs multiple segments' motion states measured by IMUs to achieve the best fit. Besides, the proposed model with different locations of an IMU showed significantly different estimation accuracy. This indicates that the segment motion states have different influences on the target variables (i.e., the vGRF and KEM). The IMU placed on the chest enabled the model to show the highest accuracy, possibly because the chest has meaningful changes of motion state and the chest (or trunk) flexion angles also affect the lower extremity biomechanics in landings [6], [36].

D. Estimation accuracy

In this work, we used accuracy distribution to assess the proposed model (Figs. 8 and 10) because the model test results have relatively large deviations in the massive test times (431 double-leg tests and 150 single-leg tests) and several outliers (The test results with $R_2 < 0.4$). Typically, the mean and standard deviation of the RMSE, rRMSE, and correlation coefficient (e.g., R^2) under k-fold cross-validation tests are used to assess machine learning models [15], [31], [37]–[39]. The statistical metrics can reflect the average performance of the models and are practical for performance comparison

between different models [31] or a model under different hyper parameter values [26]. However, it is not intuitive to reveal the performance distribution of a model via cross-validation test results, especially when the test results have large deviations and outliers. One outlier, such as a negative R^2 value, would severely debase the average R^2 and offset the statistical R^2 values. Thus, outliers should be excluded from the performance assessment and discussed individually. The outliers may suffer from accidents during the experimental testing, such as the bandage of the IMU becoming loose after intense drop landings, thereby changing the IMU positions and orientations. It was verified that the IMU positions and orientations significantly influence the accuracy of the vGRF estimation [31]. A possible solution for this is to use data augmentation techniques to induce IMU position and orientation errors and build a robust dataset for model training [40], [40]. After excluding outliers, it was found that the vGRF estimation achieved outstanding performance during single-leg drop landing when using the model with optimal IMU configurations. Half of the trials had an accuracy of more than 0.93 (RMSE and rRMSE were less than 0.21 BW and 0.06, respectively), and a quarter of the trials had an accuracy of about 0.96 (RMSE and rRMSE were less than 0.17 BW and 0.05, respectively) (Table I).

The proposed modular LSTM model outperformed the other two drop landing estimation models: acceleration-similarity and linear regression. Greenhalgh et al. [12] explored that the peak instantaneous vertical loading rates and peak tibial acceleration have a moderate Pearson correlation ($r = 0.469$). Tibial acceleration has been used to estimate the loading rate, in which the correlation coefficient is around $0.44 - 0.66$ [15]. We utilized the tibial acceleration to estimate the vGRF profile of a landing period. The correlation coefficient ($R^2 = 0.45 \pm 0.04$) is similar to the current results. The accuracy of the accelerations-similarity model is relatively low compared to the accuracy of the machine learning models (linear regression and modular LSTM models). Highly accurate estimation is necessary for the applications of retraining programs of intervention [10]. Chaaban et al. [25] used elaborated features extracted from IMU data and a linear regression model to estimate the vGRF and KEM during landing tasks. Their vGRF and KEM estimation accuracy (R^2) are 0.83 ± 0.01 and 0.64 ± 0.01, respectively. Although the vGRF estimate accuracy is promising, the KEM estimation accuracy is significantly less than that of the modular LSTM model (0.84 ± 0.12). This is because LSTM can handle the nonlinear relationship between IMU data (accelerations and angular velocities) and the KEM.

From the perspective of estimation errors, our estimations yielded relatively high RMSE values. The RMSE (mean$\pm$SD) of the vGRF (KEM) during single- and double-leg drop landings were 0.25 ± 0.13 BW and 0.18 ± 0.06 BW (0.54 ± 0.18 BW·BH and 0.38 ± 0.1 BW·BH), respectively (Table I). In a prior study [25], the mean RMSE of the peak vGRF (KEM) during double-leg landings was reported to be 0.21 BW (0.027 BW·BH). It suggested that their estimation results were acceptable since the RMSE values were smaller than clinical differences (0.24 BW and 0.035BW·BH). Here, the clinical difference indicates the vGRF or KEM difference between subjects with and without ACL reconstruction. Our model was developed to estimate the entire profile of the target variables during a drop landing period, in which the errors of the profile estimation were larger than the clinical difference. Therefore, future work should also aim to reduce the RMSE values to meet the requirements for applications of peak value estimation.

Lipps et al. [41] reported that the human knee could only withstand a load of about 4 BW within a short period before the ACL failed. The estimated vGRFs in our study were below the risky threshold of 4 BW. Lin et al. [42] performed a computer simulation study to compare lower extremity kinetics between trials with and without non-contact ACL injuries. They found that the difference in mean vGRF between injured and uninjured male subjects was 0.95 BW. In our study, the RMSE of the vGRF estimated by our model during single- and double-leg drop landings were 0.25 ± 0.13 BW and 0.18 ± 0.06 BW, respectively (Table I). The 95% limits of agreement (LoA, mean-2SD $\sim$ mean+2SD) between the estimated vGRFs and their ground truths were $-0.01 \sim 0.51$ BW and $0.06 \sim 0.3$ BW, respectively. The maximum errors of the 95% LoA were observed to be 0.51 BW and 0.3 BW for single- and double-leg drop landings, respectively. The maximum estimation errors were less than 0.95 BW. Therefore, if the difference in estimated vGRFs between two trials exceeds $0.95 + 0.51$ BW during double-leg drop landings, the trial with a higher vGRF is likely to be associated with injury. Hence, there is a high probability that the estimated vGRFs can distinguish between injured and uninjured trials in the situation. It is important to note that the estimation accuracy is not enough to distinguish any landing trials.

E. Limitations

These promising results should be interpreted in the context of several limitations associated with the study. First, this work only explored the estimation of the vGRF and KEM without considering the other dimensions: anterior-posterior and medio-lateral GRFs, knee joint abduction moments, and knee joint internal rotation moments. Estimating the lateral components of the GRF is a critical aspect when using a single-IMU approach [43]. To generalize the estimation model in more variables, the proposed modular LSTM model should be trained to predict the different dimensions of a variable in future work. Second, the model has relatively large estimation errors of the peak values (Fig. 5). This is because the variables have abrupt changes in peak points, making it relatively difficult to map the peak values than other parts. Accurately estimating the peak values is a pivot for the ACL injury risk factor assessment because the peak values normally are ACL injury risk factors. Therefore, in future work, we plan to reduce the peak value estimation errors by adding constricted conditions, such as giving higher weights to the peak value loss when training the model and setting the peak value range for the estimation. Last, the dataset was collected from male subjects without musculoskeletal disease history. It is unclear whether the model trained by the dataset can still be valid

on female subjects as well as individuals experiencing ACL reconstruction. For instance, athletes who have experienced ACL reconstruction need practical ACL risk assessment more since functional testing is needed to determine if a patient is ready to return to sports [44]. To extend the applicability of the proposed model, collecting dataset from different populations are needed in the following study. Apart from varied landing manners (toe direction), the experiment settings (landing height and distance, Fig. 3 (a)) also influence the KEM of the landings. To extend the generalization of the model in different landing height and distance, the subsequent work is to collect the dataset and assess the model under the different experiment settings.

V. Conclusion

This work proposed a modular LSTM-based model for real-time estimating the vGRF and KEM during single- and double-leg drop landings. The model has a drop landing event detection module for online identifying the ROI of the drop landing period, a time-window buffer for organizing and transferring IMU data, and four identical small-sized deep neural networks for mapping the extracted IMU data to the vGRF and KEM. The model has optimally-selected IMU configurations and LSTM unit numbers. Also, the model is modular in that it can be configured to estimate needed variables by activating its corresponding neural networks. This work, to the best of our knowledge, is the first time to investigate the real-time estimation of the vGRF and KEM during single- and double-leg drop landing tasks. This work provides an in-field and portable method to real-time quantify and monitor the vGRF and KEM during drop landings, which would contribute to widespread clinical tests for non-contact ACL injury-risk screening, evaluation of training interventions in daily-life sport, and active control of knee assistive devices.

Appendixes

TABLE II
ESTIMATION PERFORMANCE OF THE RIGHT LEG FOR THE VGRF AND KEM WITHOUT OPTIMIZED IMU CONFIGURATIONS DURING SINGLE- AND DOUBLE-LEG DROP LANDINGS. THE UNITS OF RMSE FOR VGRF AND KEM WERE BW AND BW · BH, RESPECTIVELY.

Variables	Metrics	Mean	Min	25%	50%	75%	Max
Single-leg vGRF	R^2	0.86 ± 0.12	0.30	0.85	0.91	0.94	0.98
	rRMSE	0.08 ± 0.03	0.03	0.06	0.07	0.09	0.20
	RMSE	0.28 ± 0.13	0.11	0.20	0.24	0.32	0.81
Single-leg KEM	R^2	0.81 ± 0.14	0.20	0.75	0.86	0.91	0.98
	rRMSE	0.11 ± 0.04	0.04	0.08	0.11	0.13	0.25
	RMSE	0.58 ± 0.18	0.20	0.45	0.54	0.70	1.23
Double-leg vGRF	R^2	0.79 ± 0.14	0.20	0.71	0.83	0.90	0.99
	rRMSE	0.11 ± 0.06	0.03	0.07	0.09	0.13	0.37
	RMSE	0.28 ± 0.07	0.06	0.22	0.27	0.32	0.57
Double-leg KEM	R^2	0.82 ± 0.14	0.20	0.75	0.86	0.92	0.98
	rRMSE	0.11 ± 0.04	0.04	0.08	0.10	0.13	0.28
	RMSE	0.40 ± 0.11	0.16	0.32	0.40	0.47	0.79

Acknowledgment

The authors would like to thank Kezhe Zhu for placing reflective markers during experiments and Weijia Zong for proofreading.

[1] P. Renstrom, A. Ljungqvist, E. Arendt, B. Beynnon, T. Fukubayashi, W. Garrett, T. Georgoulis, T. E. Hewett, R. Johnson, T. Krosshaug, B. Mandelbaum, L. Micheli, G. Myklebust, E. Roos, H. Roos, P. Schamasch, S. Shultz, S. Werner, E. Wojtys, and L. Engebretsen, "Non-contact ACL injuries in female athletes: an international olympic committee current concepts statement," *British journal of sports medicine*, vol. 42, no. 6, pp. 394–412, Jun. 2008.

[2] B. Fan, H. Xia, J. Xu, Q. Li, and P. B. Shull, "IMU-based knee flexion, abduction and internal rotation estimation during drop landing and cutting tasks," *Journal of biomechanics*, vol. 124, p. 110549, Jul. 2021.

[3] L.-I. Wang, "The lower extremity biomechanics of single- and double-leg stop-jump tasks," *Journal of sports science & medicine*, vol. 10, no. 1, pp. 151–156, Mar. 2011.

[4] D. A. Padua, L. J. DiStefano, A. I. Beutler, S. J. de la Motte, M. J. DiStefano, and S. W. Marshall, "The landing error scoring system as a screening tool for an anterior cruciate ligament Injury-Prevention program in Elite-Youth soccer athletes," *Journal of athletic training*, vol. 50, no. 6, pp. 589–595, Jun. 2015.

[5] H. C. Smith, R. J. Johnson, S. J. Shultz, T. Tourville, L. A. Holterman, J. Slauterbeck, P. M. Vacek, and B. D. Beynnon, "A prospective evaluation of the landing error scoring system (LESS) as a screening tool for anterior cruciate ligament injury risk," *The American journal of sports medicine*, vol. 40, no. 3, pp. 521–526, Mar. 2012.

[6] Y. Shimokochi, J. P. Ambegaonkar, E. G. Meyer, S. Y. Lee, and S. J. Shultz, "Changing sagittal plane body position during single-leg landings influences the risk of non-contact anterior cruciate ligament injury," *Knee surgery, sports traumatology, arthroscopy: official journal of the ESSKA*, vol. 21, no. 4, pp. 888–897, Apr. 2013.

[7] M. Liederbach, I. J. Kremenic, K. F. Orishimo, E. Pappas, and M. Hagins, "Comparison of landing biomechanics between male and female dancers and athletes, part 2: Influence of fatigue and implications for anterior cruciate ligament injury," *The American journal of sports medicine*, vol. 42, no. 5, pp. 1089–1095, May 2014.

[8] S. Lambrecht, A. Harutyunyan, K. Tanghe, M. Afschrift, J. De Schutter, and I. Jonkers, "Real-time gait event detection based on kinematic data coupled to a biomechanical model," *Sensors*, vol. 17, no. 4, p. 671, Mar 2017.

[9] L. Zhang, G. Liu, B. Han, Z. Wang, H. Li, and Y. Jiao, "Assistive devices of human knee joint: A review," *Robotics and autonomous systems*, vol. 125, p. 103394, Mar. 2020.

[10] R. Richards, J. C. van den Noort, M. van der Esch, M. J. Booij, and J. Harlaar, "Gait retraining using real-time feedback in patients with medial knee osteoarthritis: Feasibility and effects of a six-week gait training program," *The Knee*, vol. 25, no. 5, pp. 814–824, Oct. 2018.

[11] J. Wu, B. Becsek, A. Schaer, H. Maurenbrecher, G. Chatzipirpiridis, O. Ergeneman, S. Pané, H. Torun, and B. J. Nelson, "Real-time gait phase detection on wearable devices for real-world free-living gait," *IEEE Journal of Biomedical and Health Informatics*, pp. 1–12, 2022. [Online]. Available: 10.1109/JBHI.2022.3228329

[12] A. Greenhalgh, J. Sinclair, L. Protheroe, and N. Chockalingam, "Predicting impact shock magnitude: Which ground reaction force variable should we use?" *International Journal of Sports Science and Engineering*, vol. 6, no. 4, pp. 225–231, Dec. 2012.

[13] J. H. Zhang, W. W. An, I. P. Au, T. L. Chen, and R. T. Cheung, "Comparison of the correlations between impact loading rates and peak accelerations measured at two different body sites: Intra- and inter-subject analysis," *Gait & Posture*, vol. 46, pp. 53–56, May 2016.

[14] C. A. Laughton, I. M. Davis, and J. Hamill, "Effect of strike pattern and orthotic intervention on tibial shock during running," *Journal of applied biomechanics*, vol. 19, no. 2, pp. 153–168, May 2003.

[15] T. Tan, Z. A. Strout, and P. B. Shull, "Accurate impact loading rate estimation during running via a Subject-Independent convolutional neural network model and optimal IMU placement," *IEEE journal of biomedical and health informatics*, vol. 25, no. 4, pp. 1215–1222, Apr. 2021.

[16] G. Logar and M. Munih, "Estimation of joint forces and moments for the in-run and take-off in ski jumping based on measurements with wearable inertial sensors," *Sensors*, vol. 15, no. 5, pp. 11 258 – 11 276, May 2015.
[17] A. Karatsidis, G. Bellusci, H. M. Schepers, M. de Zee, M. S. Andersen, and P. H. Veltink, "Estimation of ground reaction forces and moments during gait using only inertial motion capture," *Sensors*, vol. 17, no. 1, p. 75, Dec. 2016.
[18] E. C.-Y. Yang and M.-H. Mao, "3D analysis system for estimating intersegmental forces and moments exerted on human lower limbs during walking motion," *Measurement*, vol. 73, pp. 171–179, Sep. 2015.
[19] P. de Leva, "Adjustments to zatsiorsky-seluyanov's segment inertia parameters," *Journal of Biomechanics*, vol. 29, no. 9, pp. 1223–1230, Sep. 1996.
[20] B. LeBlanc, E. M. Hernandez, R. S. McGinnis, and R. D. Gurchiek, "Continuous estimation of ground reaction force during long distance running within a fatigue monitoring framework: A kalman filter-based model-data fusion approach," *Journal of biomechanics*, vol. 115, p. 110130, Jan. 2021.
[21] R. Eguchi, A. Yorozu, T. Fukumoto, and M. Takahashi, "Estimation of vertical ground reaction force using low-cost insole with force plate-free learning from single leg stance and walking," *IEEE Journal of Biomedical and Health Informatics*, vol. 24, no. 5, pp. 1276–1283, May 2020.
[22] M. I. M. Refai, B.-J. F. van Beijnum, J. H. Buurke, and P. H. Veltink, "Portable gait lab: Estimating 3d grf using a pelvis IMU in a foot IMU defined frame," *IEEE Transactions on Neural Systems and Rehabilitation Engineering*, vol. 28, no. 6, pp. 1308–1316, Jun. 2020.
[23] F. J. Wouda, M. Giuberti, G. Bellusci, E. Maartens, J. Reenalda, B.-J. F. van Beijnum, and P. H. Veltink, "Estimation of vertical ground reaction forces and sagittal knee kinematics during running using three inertial sensors," *Frontiers in physiology*, vol. 9, p. 218, Mar. 2018.
[24] B. J. Stetter, F. C. Krafft, S. Ringhof, T. Stein, and S. Sell, "A machine learning and wearable sensor based approach to estimate external knee flexion and adduction moments during various locomotion tasks," *Frontiers in bioengineering and biotechnology*, vol. 8, p. 9, Jan. 2020.
[25] C. R. Chaaban, N. T. Berry, C. Armitano-Lago, A. W. Kiefer, M. J. Mazzoleni, and D. A. Padua, "Combining inertial sensors and machine learning to predict vGRF and knee biomechanics during a double limb jump landing task," *Sensors*, vol. 21, no. 13, Jun. 2021.
[26] S. Cerfoglio, M. Galli, M. Tarabini, F. Bertozzi, C. Sforza, and M. Zago, "Machine Learning-Based estimation of ground reaction forces and knee joint kinetics from inertial sensors while performing a vertical drop jump," *Sensors*, vol. 21, no. 22, Nov. 2021.
[27] S. A. Peel, T. A. Thorsen, L. G. Schneider, and J. T. Weinhandl, "Effects of foot rotation on ACL injury risk variables during drop landing," *Journal of Science in Sport and Exercise*, vol. 2, no. 1, pp. 59–68, Feb. 2020.
[28] T. Ishida, M. Yamanaka, N. Takeda, K. Homan, Y. Koshino, T. Kobayashi, H. Matsumoto, and Y. Aoki, "The effect of changing toe direction on knee kinematics during drop vertical jump: a possible risk factor for anterior cruciate ligament injury," *Knee surgery, sports traumatology, arthroscopy: official journal of the ESSKA*, vol. 23, no. 4, pp. 1004–1009, Apr. 2015.
[29] S. Marković, M. Dopsaj, S. Tomažič, A. Kos, A. Nedeljković, and A. Umek, "Can IMU provide an accurate vertical jump height estimate?" *NATO Advanced Science Institutes series E: Applied sciences*, vol. 11, no. 24, p. 12025, Dec. 2021.
[30] E. Rapp, S. Shin, W. Thomsen, R. Ferber, and E. Halilaj, "Estimation of kinematics from inertial measurement units using a combined deep learning and optimization framework," *Journal of biomechanics*, vol. 116, p. 110229, Feb. 2021.
[31] T. Tan, D. P. Chiasson, H. Hu, and P. B. Shull, "Influence of IMU position and orientation placement errors on ground reaction force estimation," *Journal of biomechanics*, vol. 97, p. 109416, Dec. 2019.
[32] T. Tan, D. Wang, P. B. Shull, and E. Halilaj, "IMU and smartphone camera fusion for knee adduction and knee flexion moment estimation during walking," *IEEE Transactions on Industrial Informatics*, pp. 1–12, 2022. [Online]. Available: 10.1109/TII.2022.3189648
[33] F. Crenna, G. B. Rossi, and M. Berardengo, "Filtering biomechanical signals in movement analysis," *Sensors*, vol. 21, no. 13, Jul. 2021.
[34] E. S. Matijevich, P. Volgyesi, and K. E. Zelik, "A promising wearable solution for the practical and accurate monitoring of low back loading in manual material handling," *Sensors*, vol. 21, no. 2, Jan. 2021.
[35] L. S. Vargas-Valencia, F. B. A. Schneider, A. G. Leal-Junior, P. Caicedo-Rodríguez, W. A. Sierra-Arévalo, L. E. Rodríguez-Cheu, T. Bastos-Filho, and A. Frizera-Neto, "Sleeve for knee angle monitoring: An IMU-POF sensor fusion system," *IEEE Journal of Biomedical and Health Informatics*, vol. 25, no. 2, pp. 465–474, Fed. 2021.
[36] A. Kulas, P. Zalewski, T. Hortobagyi, and P. DeVita, "Effects of added trunk load and corresponding trunk position adaptations on lower extremity biomechanics during drop-landings," *Journal of biomechanics*, vol. 41, no. 1, pp. 180–185, Aug. 2008.
[37] L. Tong, R. Liu, and L. Peng, "LSTM-Based lower limbs motion reconstruction using Low-Dimensional input of inertial motion capture system," *IEEE sensors journal*, vol. 20, no. 7, pp. 3667–3677, Apr. 2020.
[38] M. Gholami, A. Rezaei, T. J. Cuthbert, C. Napier, and C. Menon, "Lower body kinematics monitoring in running using Fabric-Based wearable sensors and deep convolutional neural networks," *Sensors*, vol. 19, no. 23, Dec. 2019.
[39] V. Hernandez, D. Dadkhah, V. Babakeshizadeh, and D. Kulić, "Lower body kinematics estimation from wearable sensors for walking and running: A deep learning approach," *Gait & posture*, vol. 83, pp. 185–193, Jan. 2021.
[40] C. Shorten and T. M. Khoshgoftaar, "A survey on image data augmentation for deep learning," *Journal of Big Data*, vol. 6, no. 1, pp. 1–48, Jul. 2019.
[41] D. B. Lipps, E. M. Wojtys, and J. A. Ashton-Miller, "Anterior cruciate ligament fatigue failures in knees subjected to repeated simulated pivot landings," *The American journal of sports medicine*, vol. 41, no. 5, pp. 1058–1066, May 2013.
[42] C.-F. Lin, H. Liu, M. T. Gros, P. Weinhold, W. E. Garrett, and B. Yu, "Biomechanical risk factors of non-contact acl injuries: A stochastic biomechanical modeling study," *Journal of Sport and Health Science*, vol. 1, no. 1, pp. 36–42, May 2012.
[43] A. Ancillao, S. Tedesco, J. Barton, and B. O'Flynn, "Indirect measurement of ground reaction forces and moments by means of wearable inertial sensors: A systematic review," *Sensors*, vol. 18, no. 8, Aug. 2018.
[44] K. E. Wilk, "Anterior cruciate ligament injury prevention and rehabilitation: Let's get it right," *The Journal of orthopaedic and sports physical therapy*, vol. 45, no. 10, pp. 729–730, Oct. 2015.